Supporting Online Material

Materials and Methods

Scanning Procedure. Ten right-handed subjects with no positive neuropsychiatric history provided informed consent and participated in the study. Subjects were scanned with a bite bar on a 3.0-T GE scanner. Structural images (spin echo, TR 3000 ms, TE 41 ms, FOV 20 cm, 512 x 512, ETL 8, NEX 2, 16 slices, 3 mm thick, 0 mm spacing) were perpendicular to the long axis of the hippocampus. Coplanar functional images (gradient echo, TR 3500 ms, TE 30 ms, 128 x 128, 11 slices, 116 images) were acquired during memory runs. Four subjects had participated in a previously reported study and did not require structural scanning (*S1*).

Memory Paradigm. Subjects viewed stimuli through magnet-compatible goggles (Resonance Technology, Inc.). The black-and-white faces were edited to remove all hair. During encoding, subjects viewed 8 pairs of faces and first names (4 male, 4 female) presented serially every 3.5 seconds and pressed a button for each pair. During distraction, subjects focused on a fixation cross and pressed a button when the cross changed to a circle, which occurred randomly every 2-5 seconds and lasted 0.25 seconds. During recall, subjects viewed the 8 faces serially for 3.5 seconds without the accompanying names. They attempted to recall the name and pressed a button if they judged their recall successful. Total scan duration was 406 seconds, including beginning

and ending resting blocks of 31.5 seconds. Subjects performed two to three runs with unique stimuli, and time series MR images were averaged across runs within subject. Retrieval was covert and self-monitored via button press; outside the scanner, subjects performed the same paradigm with different stimuli and overt responses to facilitate behavioral measurement. After scanning, subjects were debriefed to confirm task performance and query for strategy. Repeated measures ANOVAs identified no significant difference between performance inside the scanner compared to outside when monitored by subject ($P>0.9$) or by experimenter ($P>0.8$).

Segmentation Procedure. We estimated the location of the different architectonic subregions of the MTL by segmenting, demarcating, and unfolding structural images (*S1, S2*). After motion correction (*S3*), functional time series images were projected on the structural maps by averaging across the thickness of the cortical manifold. To facilitate high-resolution statistical computation across subjects, we registered each individual subject's images to a flat hippocampal template (*S2*) representative of our subject population (including four subjects from prior work, *S1*). The following subregion boundaries were averaged across subjects to create the flat hippocampal template: 1) Internal Border, 2) Anterior CADG - CA23DG, 3) CA23DG - CA 1, 4) CA 1 – Subiculum, 5) Subiculum - Parahippocampal/Entorhinal, 6) Posterior Collateral Sulcus, 7) Entorhinal – Perirhinal, 8) Parahippocampal - Entorhinal/Perirhinal, 9) Medial Fusiform Vertex. CA 1 = cornu ammonis 1, CA23DG = CA 2, 3 and dentate gyrus. (CADG = CA 1, 2, 3 and dentate gyrus, Sub = subiculum, PHC = parahippocampal

cortex, FG = fusiform gyrus, ERC = entorhinal cortex, and PRC = perirhinal cortex.) Second-order polynomial curves were fit to each region boundary, resampled to 100 uniformly spaced points, and vector averaged across subjects, producing an average anatomic template (Fig. 1c, *S4*). Transformations for each subject to this template were derived as follows: each of the 100 points on each boundary was perfectly displaced to match the template, and an elastic body deformation field was computed for the rest of the points to produce a field that minimizes changes in area (*S5*). Time series images were warped to the template using this transformation.

FMRI Image Analysis. To create a performance curve indicative of new learning, we assumed that a new successful retrieval is the consequence of a new successful encoding episode in the preceding encoding block. Thus, new learned pairs for a given block were calculated by subtracting total recall performance of the preceding block from the current block. For the incremental performance curve during learning, a boxcar waveform for the learn blocks was weighted by the incremental performance curve and smoothed and shifted to model typical hemodynamic response latencies (*S6*). The same procedure for the recall blocks generated a waveform for incremental recall. The flat time series were smoothed with a 5 x 5 Hanning filter (FWHM 3 mm), and pixel time courses were drift corrected with a 3rd order polynomial fit to the rest and distraction conditions. Signal intensity in each voxel and in each subject was then separately regressed against the two waveforms, and the slopes of the regressions formed two slope maps for each subject. For the random-effects calculation, a two-sided t-test compared the mean slope in each voxel

to a zero reference across subjects (n=10, *S7*).

Within the MTL, power to detect activity in some subregions (e.g. entorhinal/perirhinal cortex) can be limited by susceptibility artifact and reduced cortical thickness (*S1*). This will result in false negatives or missed activations in some subregions, making it difficult to interpret the lack of activation. Consequently, we draw conclusions only about subregions in which we have the power to detect activity in at least one contrast.

ROI Time Series Analysis. In the CA23DG, posterior subiculum, and fusiform gyrus of every subject, time courses were averaged across all voxels and both hemispheres without pixel selection and drift corrected with a 3rd order polynomial. The posterior subiculum was defined as all subicular voxels posterior to the midpoint between the most anterior and most posterior subicular pixel in flat space. Regression and random effects calculations were separately performed with the incremental learning, incremental recall, and memory boxcar (contrasting learn and recall versus distraction and rest) waveforms. Paired t-tests and a three-way ANOVA compared the mean slope in each subregion either to a zero reference or to another subregion's slopes across subjects.

Hemispheric Comparison. Two-sided paired t-tests found no significant left-versus-right difference in slope maps for incremental learning in CA23DG (p=0.155), incremental recall in the posterior subiculum (p=0.984), and the memory boxcar in the fusiform gyrus (p=0.121).

3-D Visualization. Each voxel in flat space has an X, Y, and Z coordinate corresponding to 3-D space. Flat images of the X, Y, and Z ordinate (where intensity in flat space represents the corresponding coordinate value in 3-D space) were made in the left hemisphere of each subject. These flat coordinate images were warped into the atlas space and averaged across subjects (*S5*). By tracing through these average coordinate images we constructed a 3-D mesh onto which we superimposed the positively active voxels from the incremental learning and recall contrasts at a t threshold of 2.4.

Whole Brain Imaging. Seven of the 10 subjects were also scanned with whole-brain structural (spin echo, TR 4000 ms, TE 54 ms, FOV 20 cm, 128 x 128, NEX 4, 29 slices, 4 mm thick, 1 mm spacing) and coplanar functional imaging (gradient echo, TR 3500 ms, TE 45 ms, 64 x 64, 18-21 slices, 116 images). After motion correction (*S4*), normalization (*S8*), and gaussian smoothing (FWHM 6 mm), we imported the data into SPM'99 (Wellcome Department of Cognitive Neurology, London, UK; www.fil.ion.ucl.ac.uk) and computed a recall contrast using total recall performance as a covariate. We then computed a t-map of the performance covariate (p=0.00001, uncorrected, spatial extent 10 voxels).

Figures

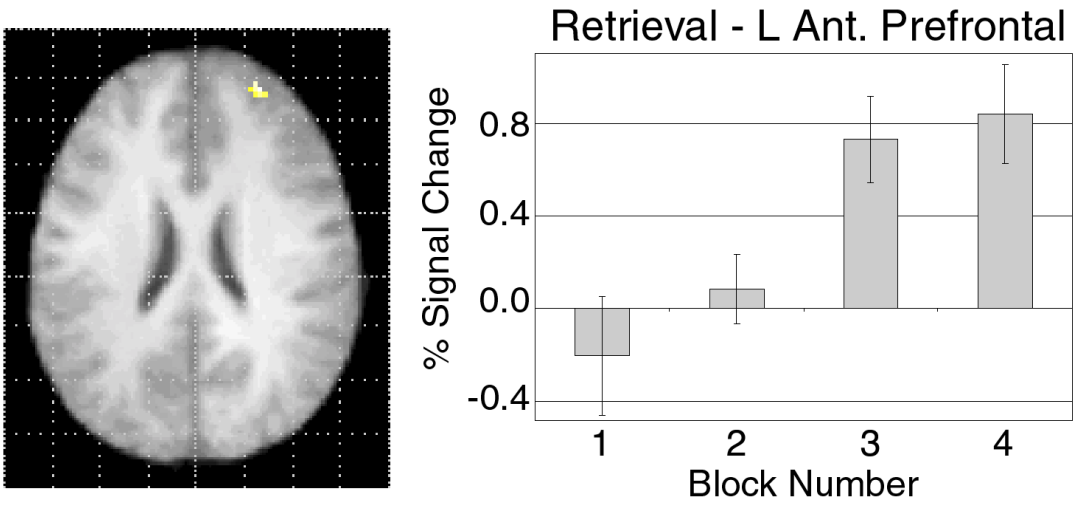

Figure S1. Statistical Parametric Mapping showing signal change in the left anterior prefrontal cortex correlated with increasing recall. The activation map superimposed on the T1 image is in radiological format (the right side of screen corresponds to the left side of the brain). The time course of left anterior prefrontal cortex, BA 10 (-26, 52, 24), was extracted using SPM's VOI feature (radius 5 mm). Other activation foci were right BA 37 (22, -48, -14), left BA 39 (-54, -68, 14), left BA 4 (-48, -16, 40), left BA 6 (-6, -8, 50), and left BA 19 (-32, -56, 6).

References

1. M. Zeineh, S. Engel, S. Bookheimer, *NeuroImage* **11**, 668 (2000).
2. M. Zeineh, S. Engel, P. Thompson, S. Bookheimer, *The Anatomical Record (New Anat.)* **265**, 111 (2001).
3. R. Woods, S. Grafton, C. Holmes, S. Cherry, J. Mazziotta, *J. Comp. Assist. Tomog.* **22**, 139 (1998).

4. P. Thompson, R. Woods, M. Mega, A. Toga, *Human Brain Mapping* **9**, 81 (2000).
5. P. Thompson, A. Toga, in *Brain Warping* A. W. Toga, Ed. (Academic Press, San Diego, 1998) pp. 311.
6. M. Cohen, *NeuroImage* **6**, 93 (1997).
7. A. Holmes, K. Friston, *NeuroImage* **7**, S754 (1998).
8. R. Woods, M. Dapretto, N. Sicotte, A. Toga, J. Mazziotta, *Human Brain Mapping* **8**: 73 (1999).